



Shahrood University of  
Technology



Iranian Society of  
Mining Engineering  
(IRSM)

## An Investigation into Bench Health Monitoring under Blast Loading in Hoek-Brown Failure Criterion using Finite Difference Method

Seyed Ahmad Mousavi<sup>1</sup>, Kaveh Ahangari<sup>1\*</sup>, and Kamran Goshtasbi<sup>2</sup>

1. Department of Mining Engineering, Science and Research Branch, Islamic Azad University, Tehran, Iran

2. Department of Mining Engineering, Faculty of Engineering, Tarbiat Modares University, Tehran, Iran

### Article Info

Received 10 July 2022

Received in Revised form 27  
August 2022

Accepted 7 September 2022

Published online 7 September  
2022

DOI: [10.22044/jme.2022.12094.2207](https://doi.org/10.22044/jme.2022.12094.2207)

### Keywords

Disturbance factor

Bench health monitoring

Hoek-Brown failure criterion

Peak particle velocity

Plastic zone

### Abstract

Blast and stress release create cracks, fractures, and excavation damage zone in the remaining rock mass. Bench health monitoring (BHM) is crucial regarding bench health and safety in blast dynamic loading. Several empirical criteria have been proposed for a quick estimation of different parameters of a rock mass in the zone damaged by the blast. This work estimates the rock mass properties behind the blast hole based on the generalized Hoek-Brown failure criterion and quantitative disturbance factor (D). Considering a constant D value, either zero or one, for the entire rock mass, remarkably alters its strength and stability, resulting in very optimistic or very conservative analyses. Therefore, D is considered based on the elastic damage theory, and numerical simulation is conducted based on the finite difference software FLAC to investigate the vibration and damage threshold by monitoring the peak particle velocity (PPV) in the bench domain with different geometries. According to the numerical simulation, as the depth behind the blast hole increases, the value of D decreases from one to zero almost non-linearly, resulting in a non-linear reduction in the Hoek-Brown behavioral model properties. It is found that using various parameters of rock mass in the blast-induced damage zone behind the hole leads to thoroughly different PPV values than the constant parameters. Accordingly, the approach to using the quantified values of parameter D is of great importance in the estimation of various properties of a rock mass in the blast-induced zone, as well as calculation of the vibration.

### 1. Introduction

The drilling and blasting method is an approach for rock excavation in the slopes and underground structures. Shock waves and high-pressure gases are produced due to the blasting create, and propagate the cracks and fractures in the rock mass, consequently resulting in rock fragmentation [1-3]. Additionally, vibrations or waves are among the main problems and consequences of blasting in mines, which may lead to the opening and slippage of joints and faults in the rock mass, and damage to benches and the surrounding structures, along with the economic and environmental issues [4-10]. The unwanted damaged regions of rocks in surface blasting can be divided into two groups: over-break zones (as back-breaks and side-breaks) and cracked zones. Unwanted damages to benches and

slopes are called blast-induced rock mass damages. These damages reduce the rock mass integrity, on the one hand, and result in the excavation problems, slope instability, and inappropriate reduction of the bench width, on the other hand; accordingly, controlling ground vibrations, calculating damage size in the rock mass, and minimizing the blast-induced damages are of crucial importance [11-13]. Various indices have been introduced to investigate blast-induced vibration effects, among which the peak particle velocity (PPV) has received attention from many researchers, and a variety of relationships have been presented to relate PPV with the blasting zone properties and enhance it using different methods [14, 15]. Many researchers have predicted the

✉ Corresponding author: [kaveh.ahangari@gmail.com](mailto:kaveh.ahangari@gmail.com) (K. Ahangari).

blast-induced damaged zone regarding the PPV threshold [4, 12, 16, 17]. Shadabfar *et al.* [18] have provided comprehensive modeling based on mathematical fundamentals and improvements in the current criteria to determine the extent of damage due to the single-hole blasting using the probabilistic method.

In the zones of blast-induced damage, the rock mass properties are reduced, so the effects of the weakened rock mass on estimating ground vibration and slope stability are critical. Moreover, if such a rock mass is assumed to be intact, the slope stability will be overestimated. A realistic analysis of the ground vibration and mine wall stability after blasting is possible if one can estimate the rock mass strength reduction caused by blasting [19-21]. As it is evident, the most accurate method for obtaining the rock mass properties is large-scale in-site experiments in the field [22, 23]. However, the probably sloped conditions and high elevation of the benches, along with the costly and lengthy experiments, make their use difficult. Several empirical criteria have been proposed for a quick estimation of the parameters of a rock mass. In this regard, the Hoek-Brown failure criterion is an accepted method in the community of rock mechanics [24]. A parameter called the disturbance factor was introduced to improve the strength estimation accuracy of a rock mass regarding the blast-induced strength reduction and stress relaxation during excavations. The disturbance factor allows for the quick estimation of the rock mass properties in the excavation damage zone [24, 25].

In the guidelines of the Hoek-Brown criterion, a constant disturbance factor has been assigned to damaged rock masses without considering the damage reduction with the rise in the depth behind slope surfaces and holes [25-27]. Some researchers considered assigning a variable disturbance factor to the zone behind the slope surfaces since assigning a constant disturbance factor to the damaged zone is not proper. For instance, some of them assumed a decreasing linear disturbance factor and a parallel layer model [19, 21, 28, 29]. Through numerical simulations, Lupogo *et al.* [30] and Rose *et al.* [31] have found that the damage declines almost exponentially with the rise in depth. Lemaitre [32] has presented some equations, defined as the relative value of the elastic modulus damage, based on elastic damage theory to quantify the disturbance factor. Hamdi *et al.* [33], Chen *et al.* [34], Pan *et al.* [16], and Wang *et al.* [35] have employed the relative value of elastic modulus damage for numerical modeling. Yang *et*

*al.* [36] have utilized the P-wave velocities of the rock masses based on the Hoek-Brown criterion and the rock mass quality Q-system to develop the quantity of the disturbance factor. Regarding the previous discussions and the importance of blast-induced zone characterization and reduction in rock mass properties in this zone, in this research work, bench health monitoring (BHM) will be conducted through numerical simulation of the PPV threshold in the FLAC finite difference software.

## 2. Methodology

### 2.1. Generalized Hoek-Brown failure criterion

Following their study on the non-linear Griffith failure criterion regarding the tensile fracture of fragile materials such as glasses, Hoek and Brown proposed the empirical equation below with the results of a wide range of triaxial experiments on the intact rock samples to perform the required analyses of underground excavations designed in hard rock masses [24, 37]:

$$\sigma_1 = \sigma_3 + \sigma_{ci} \sqrt{\left(m_i \frac{\sigma_3}{\sigma_{ci}} + 1\right)} \quad (1)$$

where  $\sigma_1$  and  $\sigma_3$  are the major and minor principal stresses in failure, respectively. Moreover,  $\sigma_{ci}$  is the unconfined compressive strength of the intact rock, and  $m_i$  is the Hoek-Brown constant for the intact rock, which depends on the rock type, the mineral composition, and the texture size.

The Hoek-Brown failure criterion for the rock mass was updated in numerous editions with fundamental changes in the concepts and equations from 1965 to 2018. These changes included the definition of the undisturbed and disturbed rock mass and the zero tensile strength for poor rock masses. Furthermore, in order to connect this criterion to geological observations by one of the rock mass classification systems, the geological strength index (GSI) was introduced instead of Bieniawski's rock mass rating (RMR) [27, 38].

The generalized Hoek-Brown criterion for estimating the rock mass strength is defined as below:

$$\sigma'_1 = \sigma'_3 + \sigma_{ci} \left( m_b \frac{\sigma'_3}{\sigma_{ci}} + s \right)^a \quad (2)$$

where  $m_b$ ,  $s$ , and  $a$  are the Hoek-Brown constants for the rock mass, and can be calculated based on

the latest presented edition using the below equations:

$$m_b = m_i \exp\left(\frac{GSI - 100}{28 - 14D}\right) \quad (3)$$

$$s = \exp\left(\frac{GSI - 100}{9 - 3D}\right) \quad (4)$$

$$a = \frac{1}{2} + \frac{1}{6}(e^{-GSI/15} - e^{-20/3}) \quad (5)$$

For undisturbed rock,  $a = 0.5$ ,  $s = 1$ , and  $D$  is a factor that depends on the level of disturbance due to the blasting or stress relaxation, which will be discussed in Section 2-2 [25]. This study aims to investigate the disturbance factor ( $D$ ) variations behind the blast hole and its effect on the rock mass properties and bench health monitoring (BHM). Therefore, the details of the other parameters of the Hoek-Brown criterion in Eqs. 2-4 are available in Hoek [39].

The Hoek-Brown criterion also provides estimations of the rock mass deformation modulus ( $E_{rm}$ ), uniaxial compressive strength ( $\sigma_{cm}$ ), and uniaxial tensile strength ( $\sigma_{tm}$ ) as the following equations [25, 40]:

$$E_{rm} = E_i \left(0.02 + \frac{1 - D/2}{1 + e^{((60+15D-GSI)/11)}}\right) \quad (6)$$

$$\sigma_{cm} = \sigma_{ci} \times \frac{(m_b + 4s - a(m_b - 8s))(m_b / 4 + s)^{a-1}}{2(1+a)(2+a)} \quad (7)$$

$$\sigma_{tm} = \frac{s\sigma_{ci}}{m_b} = \frac{\sigma_{ci}}{m_i} \cdot \exp\left[\frac{(GSI-100).(19-11D)}{(9-3D).(28-14D)}\right] \quad (8)$$

where  $E_i$  is the intact rock deformation modulus (MPa).

## 2.2. Disturbance factor (D) of Hoek–Brown criterion

The rock mass strength parameters can be changed due to the stress relaxation and depending on the excavation type and blasting quality control. This impact is applied using the disturbance factor ( $D$ ). The blast disturbance factor was introduced in the 2002 edition of the Hoek-Brown criterion to estimate its parameters including strength and deformation modulus. The value of  $D$  ranges from zero for in-site intact rock masses to one for very disturbed rock masses [25].

The experiences of slope design in huge open-cast mines have shown that the Hoek-Brown criterion of undisturbed in-situ rock masses ( $D = 0$ ) leads to very optimistic parameters. Most of these studies have revealed that when assuming undisturbed conditions, the predicted Hoek–Brown strength is significantly higher than the back-calculated strength values. Heavy blasting and stress relaxation create disturbance in the rock mass. It is more suitable to employ the disturbed rock mass parameters ( $D = 1$ ) in the Hoek-Brown criterion for these rock masses. Some guidelines have been provided for estimating the disturbance factor for tunnels and slopes. Primary guidelines have also been presented as the starting point for determining the thickness of the blast damage zone due to the production blasting [25, 27, 40].

In Figure 1, the ranges between the blast-damaged rock mass, muck pile, and undisturbed rock mass are schematically presented. The damaged rock mass properties affect the slope stability after excavation of the muck pile. The blast damaged zone thickness ( $T$ ) depends on the blasting operations [26]. When blasting is confined with little or no control,  $T = 2.0-2.5 H$ . When blasting is toward the free face with no control,  $T = 1.0 - 1.5 H$ . When the blasting is toward the free face with some controls, e.g. several buffer rows are used,  $T = 0.5 - 1.0 H$  [20, 26]:

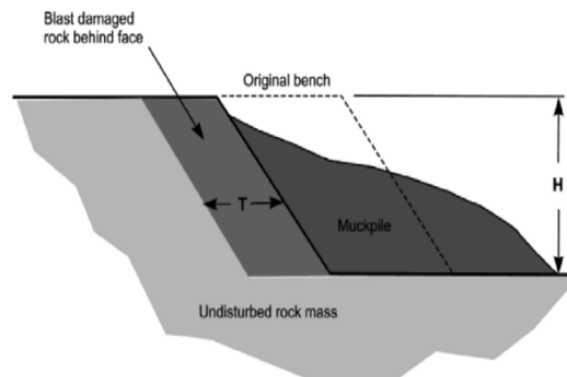
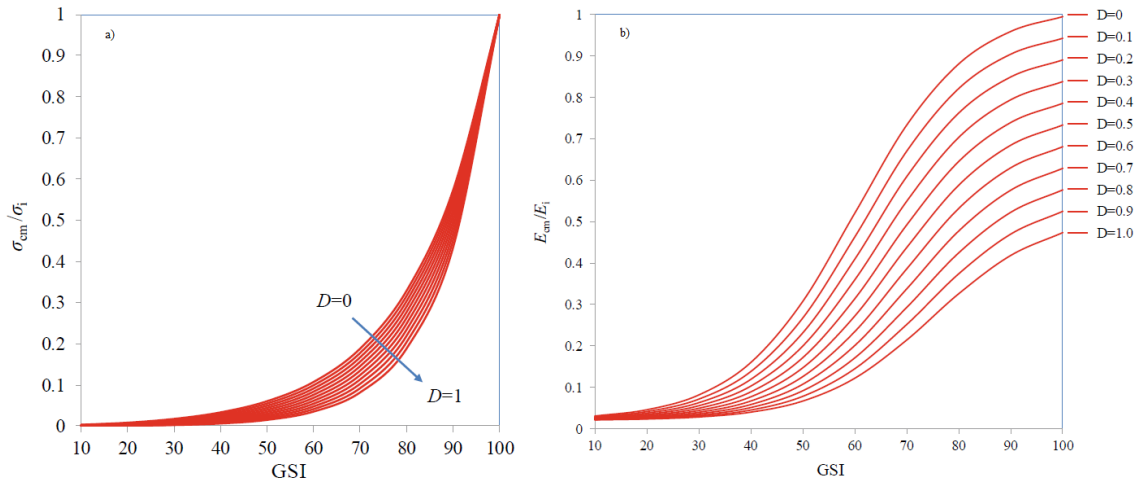


Figure 1. Schematic representation of undisturbed, disturbed, and blasted rocks in a mine wall [26].

Different factors such as blasting design and rock mass properties might affect the disturbance factor in a rock mass, so the accurate determination of the D value is not simple.

The rock mass properties in the damaged zone are lower than in the undamaged zone [25]. By performing a sensitivity analysis, it can be determined how significant the D impact is on the

properties of the rock mass and slope design. Figs. 2(a) and 2(b) illustrate the D impact on the compressive strength and deformation modulus of the rock mass, respectively. It is obvious that D has a considerable impact on the estimated deformation modulus and compressive strength of the rock mass [26, 40, 41].



**Figure 2. Impact of disturbance factor (D) on compressive strength (a) and deformation modulus (b) of rock mass [41].**

Selecting a suitable value and determining the expansion of the damaged zone are two principal matters in employing the D factor. The most important point in determining the expansion of the blasting damage is that the D factor should not be employed for the whole rock mass near the blasting. This is a prevalent modeling mistake that can remarkably underestimate the rock strength and the ultimate wall stability. The D factor should only be considered for the damaged zone of the rock [26].

### 2.3 Accumulative damage from blasting

Considering the damage as isotropic is among the simplest but the most prevalent hypotheses in continuum damage mechanics [33, 35]. By applying the blasting stress, primary cracks of the rock mass can be activated. Then they start to be propagated, and D starts to rise. The activated rock mass cracks propagate continuously, resulting in new damages. In this case, D should be considered an internal state variable, which indicates the rock mass damage level at each instant, and a comprehensive description of the rock mass requires a method showing the growth and temporal change of damages in the rock mass. Therefore, there would be accumulative blasting damage ( $D_n$ ) [35].

Based on effective stress, Lemaitre showed the isotropic distribution of micro-cracks and damages in materials as the reduction in the elastic modulus. A partly damaged rock is deformed under tensile loads with an  $E_1$  deformation modulus, which is smaller than the  $E_0$  primary modulus of the intact rock. The disturbance factor of  $D_n$  is considered a parameter that reduces the material's modulus from the primary modulus to the  $E_1$  modulus, as follows [16, 32-35]:

$$D_n = 1 - \frac{E_1}{E_0} \tag{9}$$

As mentioned in the previous section, in a numerical simulation, the disturbance factor should not be taken as a constant value between zero and one but rather should be taken into account using the quantitative equations available. In this research work, Eq. 9 was used. Therefore, in the numerical modeling, the value of  $D_n$  should be assigned to each element, the model should be updated in each time step compared to the damage in the previous run, and finally, all Hoek-Brown parameters related to the disturbance factor including  $m_b$ ,  $s$ , and  $E$  should be updated and decreased only in the damaged zone during the run according to Eqs. 10-12. Consequently, the  $\sigma_c$  and

$\sigma_t$  parameters are also updated, which is the advantage of this approach over the method that weakens the entire model.

$$m_{bu} = m_i \exp\left(\frac{GSI - 100}{28 - 14D_n}\right) \quad (10)$$

$$s_u = \exp\left(\frac{GSI - 100}{9 - 3D_n}\right) \quad (11)$$

$$E_{rm} = E_i \left(0.02 + \frac{1 - D_n/2}{1 + e^{((60+15D_n-GSI)/11)}}\right) \quad (12)$$

#### 2.4. Calculation of PPV and determination of damage threshold

The most common method for measuring blast-induced damage is to measure vibrations that result from blasting. The ground vibration recording devices can directly measure the peak particle acceleration (PPS) as well as peak particle velocity (PPV). The two types of sensors of the geophone and accelerometer can be used for blasting. The accelerometers are mainly used in the near-field areas of blasting, and by using them, the acceleration can be directly measured. Meanwhile, in the far-field areas of blasting, geophones are mostly used, and by using them, the velocity can be directly measured. PPV not only theoretically corresponds to the blast-induced stress, but it also has a proper correlation with the real damage level, and is simpler than the other methods in terms of operations and also more accessible. PPV is obtained from Eq. 13 [17]:

$$PPV = \sqrt{(V_{\max})_x^2 + (V_{\max})_y^2 + (V_{\max})_z^2} \quad (13)$$

where  $V_x$ ,  $V_y$ , and  $V_z$  are the longitudinal, vertical, and transversal components of PPV (mm/s).

The PPV threshold is significantly affected by the blasting load and the rock mass properties. Therefore, obtaining an accurate value is very difficult. Numerous researchers have used PPV in the field tests and numerical analyses, proposing different values for the PPV threshold [16, 18].

As a result, PPV was used as the main parameter for the investigation of the effects of blasting disturbance factor (D) and bench health monitoring (BHM). According to Bihandri [42], the PPV threshold value of PPV = 50 mm/s was considered for the damage threshold. Therefore, after applying

the blasting load to the model and updating the parameters of the Hoek-Brown failure criterion in the damaged zone, monitoring the PPV value was performed using the FISH program in the FLAC software for the considered recorded points.

In this work, we have two important FISH programs: 1- regarding the PPV calculation, 2- regarding the calculation of blasting disturbance factor (D) and updating the parameters of the Hoek-Brown criterion. For the FISH program regarding PPV: PPV is the average value of the longitudinal, vertical and transversal velocity, and it is calculated using Eq. 13. First, certain key points in the grid must be identified and selected, and then using pre-defined variables related velocity, the PPV value is obtained. It is necessary that the maximum PPV value is selected WHILE-STEPPING. To do this, initially the PPV value is assigned to an extra variable, and using the IF statement, the obtained velocity value is compared with the value assigned to the extra variable. If a higher value is recorded, that number is considered as the final PPV value.

For the FISH program regarding the D parameter: The value of D is obtained from Eq. 9. Before the explosion, the rock mass deformation modulus is a constant, defined value that is presented in Table 1 and is assigned to the model in the static solution single. The corresponding FISH variables to directly calculate the post-explosion rock mass deformation modulus for each of the zones in the model are not available. Therefore, we can calculate the value of the shear modulus or the bulk modulus for each zone using the FISH variables related to stress and strain, and then calculate the deformation modulus of each zone using the existing equations for elasticity. Finally, the D value of each zone can be calculated. Additionally, a function of all of the parameters in the Hoek-Brown criterion that relate to the disturbance factor including  $m_b$ ,  $s$ ,  $E$ ,  $\sigma_c$ , and  $\sigma_t$  is created, and the values are updated during the run and WHILE-STEPPING.

### 3. Numerical Modeling Considerations

#### 3.1. Geometry and model properties

For bench health monitoring (BHM), first, the monitoring goals should be determined regarding the requirements of rock engineering challenges and the use of micro-seismic monitoring. Then the whole region involved can be evaluated based on the monitoring goals. The sensitivity extent and location accuracy in the monitored areas depend on the possibility and severity of the rock mass

instability in each area. Micro-seismic monitoring should be more sensitive and have a higher location accuracy when the likelihood of rock mass instability is greater. According to the International Society for Rock Mechanics (ISRM), as shown in Figure 3, for engineering monitoring of the slope, the sensors are directly installed in the slope body, where some concerns exist about the slope surface [43].

In this work, the total number of created models was 90, which consisted of three benches of 5-, 10-

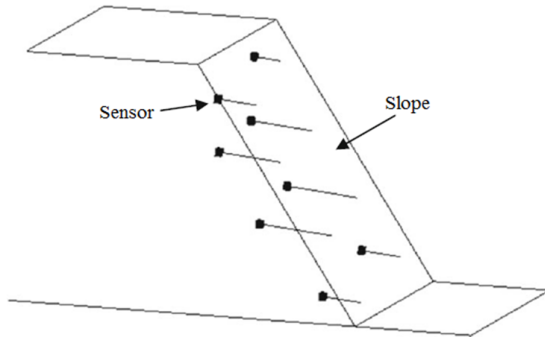


Figure 3. Layout of sensors for micro-seismic monitoring of rock mass fracturing in slope engineering [43].

, and 15-meters height and three slope angles of 55, 65, and 75 degrees, and various widths (the distance between the hole and the bench toe above) from 1 to 10 m, which are schematically shown in Figure 4.

Moreover, in this work, the rock mass properties were extracted from the values presented by Hoek and Brown [44] for granites. For the rock mass behavior modeling, the modified Hoek-Brown model was used. The rock mass properties are presented in Table 1.

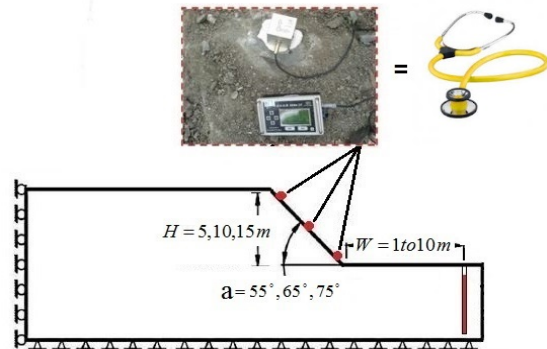


Figure 4. Geometric variables used in numerical analysis.

Table 1. Details of dynamic properties of granite rock mass [44].

D	Density(Kg/m <sup>3</sup> )	m <sub>i</sub>	GSI	m <sub>b</sub>	s	a	σ <sub>tm</sub> (Pa)	σ <sub>cm</sub> (Pa)	E <sub>rm</sub> (Pa)
0	2700	25	75	10.23	0.062	0.501	1.69E+06	1.28E+08	8.16E+10
1	2700	25	75	4.19	0.015	0.501	1.03E+06	7.96E+07	2.70E+10

### 3.2. Damp and mesh parameters

One of the crucial problems concerning meshing in dynamic analyses is determining the proper mesh size to control wave transmission. The frequency and velocity of the applied wave to the system are two parameters affecting the numerical computation accuracy of the wave propagation. Kuhelemeyer and Lysmer [45] showed that to ensure the correct wave transmission and rational analysis of the wave propagation using the numerical method, the largest dimension of the element ( $\Delta l$ ) must be lower than one-tenth to one-eighth of the created wavelength by the highest input wave frequency to the medium [46], i.e.:

$$\frac{\lambda}{10} \leq \Delta l \leq \frac{\lambda}{8} \tag{14}$$

where  $\lambda$  is the wavelength created by the largest frequency component of the waves entering the system, which can create energy.

On the other hand, considering the geo-mechanical parameters of the medium, the

compressive ( $C_p$ ) and shear ( $C_s$ ) wave velocities are obtained using the following equations [45, 46]:

$$C_p = \sqrt{\frac{K + 4G/3}{\rho}} \tag{15}$$

$$C_s = \sqrt{\frac{G}{\rho}} \tag{16}$$

where K is the bulk modulus, G is the shear modulus, and  $\rho$  is the density of the medium. By substituting the elastic properties of the most critical state of the medium, i.e. the rock mass properties corresponding with D = 1 from Table 1 in the equations above, the compressive and shear wave velocities were calculated at 3333.3 and 2041.2 m/s, respectively. The mesh size was almost 2 meters, and since the smaller mesh sizes lead to increased accuracy in software's calculations, so we considered the mesh size to 0.5 m for more accuracy.

### 3.3. Boundary conditions and mechanical damping

Boundary condition and mechanical damping are aspects that the user should consider when preparing the FLAC model for dynamic analysis. In a FLAC dynamic analysis, two boundary conditions are usually used. One is the free-field boundary, and the other is the quiet (viscous) boundary. The wave reflections at model boundaries may be reduced by specifying the boundary conditions. The quiet boundary is based on the use of independent dashpots in the normal and shear directions at the model boundaries. The quiet boundary prevents the reflection of outward-propagating waves back into the model and allows the necessary energy radiation. The free-field boundary enforces free-field motion at the lateral boundaries of the model such that these boundaries retain their non-reflecting properties (i.e. outward waves are properly absorbed). In FLAC, the free-field boundaries are coupled with viscous dashpots to simulate a quiet boundary [46]. Since quiet boundaries are best-suited when the dynamic source is within a grid [46], the quiet boundary conditions are employed for the lateral and bottom boundaries of the model to avoid unwanted reflection of the blasting wave into the model. Moreover, based on the term “Burden”, which is defined as the distance from the front row of holes to the free surface, the right-lateral boundary of the model is also considered as the free. The main goal of applying these boundaries is to allow the expansion to occur only in free surface.

Types of damping include viscous and hysteretic damping. In rock and soil, natural damping is mainly hysteretic. Hysteretic damping is independent from frequency, and assumes non-linear relationships between stress-strains. Viscous damping is frequency-dependent. Rayleigh damping is viscous damping, which is proportional to a linear combination of mass and stiffness.

In time-domain programs, Rayleigh damping is commonly used to provide damping. Rayleigh damping is specified in FLAC with the parameter center frequency (cycles per second) and critical damping ratio. In this work, the Rayleigh damping,

which is often used for dynamic geo-technical engineering, is employed. For geological materials, the damping ratio commonly falls in the range of 2-5% of critical. In the analyses that use one of the plasticity constitutive models like the Hoek-Brown criterion, a considerable amount of energy dissipation can occur during plastic flow. Thus for many dynamic analyses that involve large-strain, only a minimal percentage of damping (e.g. 0.5%) may be required. Therefore, in this work, the damping ratio was considered to be 0.5% in the conducted modeling [46].

### 3.4. Blast loading

During the blasting process, the medium is loaded in two steps approximately. In the first step, the loading is performed by the impact wave. The expansion caused by the blasting gases results in the reloading on the surrounding medium in the second step. The present work focuses on the value of vibration caused by a single-hole pattern and a single explosion stage. Moreover, since no delays are taken into account, the blast loading is among the crucial parameters influencing the vibration recorded on the bench slope. A single hole with a diameter of 200 mm and a burden of 2 meters was considered. The explosive was ANFO with a detonation velocity of 4160 m/s and an explosive density of 0.931 gr/cm<sup>3</sup> [47]. The maximum dynamic pressure applied to the whole blast hole wall (the hole pressure) was calculated using Eqs. 17-20. Its advantage is the use of the properties of rock mass and explosives for calculating the blasting pressure [4, 17].

$$PD = 432 \times 10^{-6} \frac{\rho_e \cdot VD^2}{1 + 0.8\rho_e} \tag{17}$$

$$PE = \frac{1}{2} PD \tag{18}$$

$$PW = PE \cdot \frac{1}{2} \left(\frac{r_h}{b}\right)^{-qk} \tag{19}$$

---


$$P(t) = PW \cdot \frac{8\rho_r \cdot C_p}{\rho_r \cdot C_p + VD \cdot \rho_e} \left[ e^{-\beta t / \sqrt{2}} - e^{-\sqrt{2}\beta t} \right] \quad \& B = 16338 \tag{20}$$


---

In these equations, PD is the blasting pressure (MPa),  $\rho_e$  is the explosive density (g/cm<sup>3</sup>), q is the specific heat coefficient, k is the explosive shape

factor (2 for cylindrical charges and 3 for spherical charges),  $r_h$  is the blasting hole radius (mm), b is the explosive radius (mm),  $\rho_r$  is the rock density

( $\text{gr}/\text{cm}^3$ ),  $VD$  is the detonation velocity (m/s), and  $t$  is time (s).

The maximum dynamic pressure was calculated at 4.45 GPa by substituting the above parameter values in Eq. 20. Since explosive blasting is a complex instantaneous process, for simplifying the analysis in this work, the blasting load was applied as a triangle pulse time history curve to the model, as shown in Figure 5, i.e. the load rises linearly to the highest load in the first  $20 \mu\text{s}$  before unloading, and then the linear drop of the pressure lasts  $250 \mu\text{s}$ .

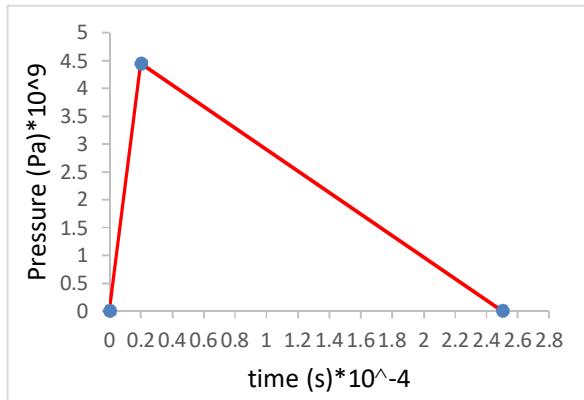


Figure 5. Time history diagram of equivalent load.

#### 4. Results and discussion

##### 4.1. Effect of disturbance factor (D)

The present work investigated three different types of models, namely models with the Hoek-

Brown constant parameters  $D = 0$  and  $D = 1$  according to Table 1, as well as a model applying the  $D = f$  function from Eq. 9. First, the PPV values from the hole-head to the toe of the above bench (history points from a to u) with a distance of 50 cm were monitored. Figure 6 illustrates that with the rise in the distance from the hole, the PPV value decreases, showing the wave damping. Furthermore, the PPV values recorded for the model with  $D = 0$  were lower than those for the model with  $D = 1$ , and in the model where the  $D$  value was assigned as a function, the recorded values differed from those of the two mentioned models. This shows that if we weaken the model's mechanical properties by applying  $D = 1$ , higher vibration values will be recorded in the model. This weakening may have lower correctness in terms of numerical modeling, and the analyses may be conservative. In case the mechanical properties of the model are investigated by applying the parameters corresponding with  $D = 0$ , lower vibration values may be recorded, i.e. the analyses may be optimistic. Therefore, by assigning Eq. 9 to the model as fish programming and allowing the model to apply the  $D$  value during the run and reduce and apply other parameters depending on the  $D$  of the Hoek-Brown criterion during the run only for the damaged zone, more rational values of PPV will be obtained. Accordingly, the other models were developed by applying the function for  $D$ .

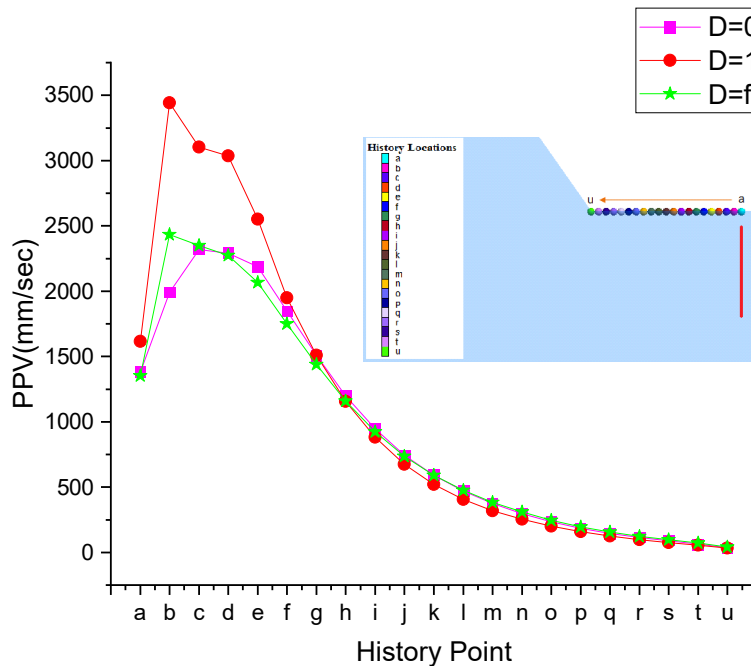


Figure 6. PPVs recorded in two models of rock masses with  $D = 0$  and  $D = 1$ , compared to a model with  $D = f$ .

### 4.2. Estimation of rock mass properties in blast-induced damaged zone

Primary values of the rock's dynamic properties, i.e.  $D = 0$  from Table 1 were applied to the model. The  $D$  value was applied to the model as the function mentioned in Section 3-2 using fish programming in the FLAC software. The zones of the model with a deformation modulus lower than the primary deformation modulus of the rock mass were known as the blast-induced damaged zone.

Some of the factors directly related to the disturbance factor in the Hoek-Brown failure criterion are deformation modulus  $E$ ,  $m$ , and  $s$  parameters. These parameters are reduced with the increment of the disturbance factor, and the tensile and compressive strength values are reduced indirectly. All these parameters, which are the inputs to the Hoek-Brown criterion, are updated in each time step during the run by fish programming in the FLAC software. The parameters are reduced in the damaged zone, and in areas out of this zone,

the primary values of properties are preserved ( $D = 0$ ).

Figure 7(a) depicts the Hoek-Brown disturbance factor ( $0 < D < 1$ ) due to the blasting behind the blasting hole. In Figure 7(b), we can observe that in areas near the hole where the blasting load is higher area and in damaged zones, the rock mass deformation modulus  $E_{rm}$  is lower, and it increases to the undisturbed value  $E_{rm0}$  with the rise in the hole distance. At distances closer to the hole, where the rock mass experiences the most severe damage ( $D = 1.0$ ), the deformation modulus is reduced to 0.33 compared to the damaged value. Moreover, Figs. 7(c-f) show the  $m_b / m_0$ ,  $s / s_0$ ,  $\sigma_{crm} / \sigma_{crm0}$ , and  $\sigma_{trm} / \sigma_{trm0}$  ratios between the disturbed and undisturbed rock masses, which are 0.41, 0.25, 0.62, and 0.61, respectively. The  $s$  parameter of the Hoek-Brown criterion is weakened due to the excavation damages caused by more blasting and has the highest effect, while the rock mass compressive strength has the lowest impact.

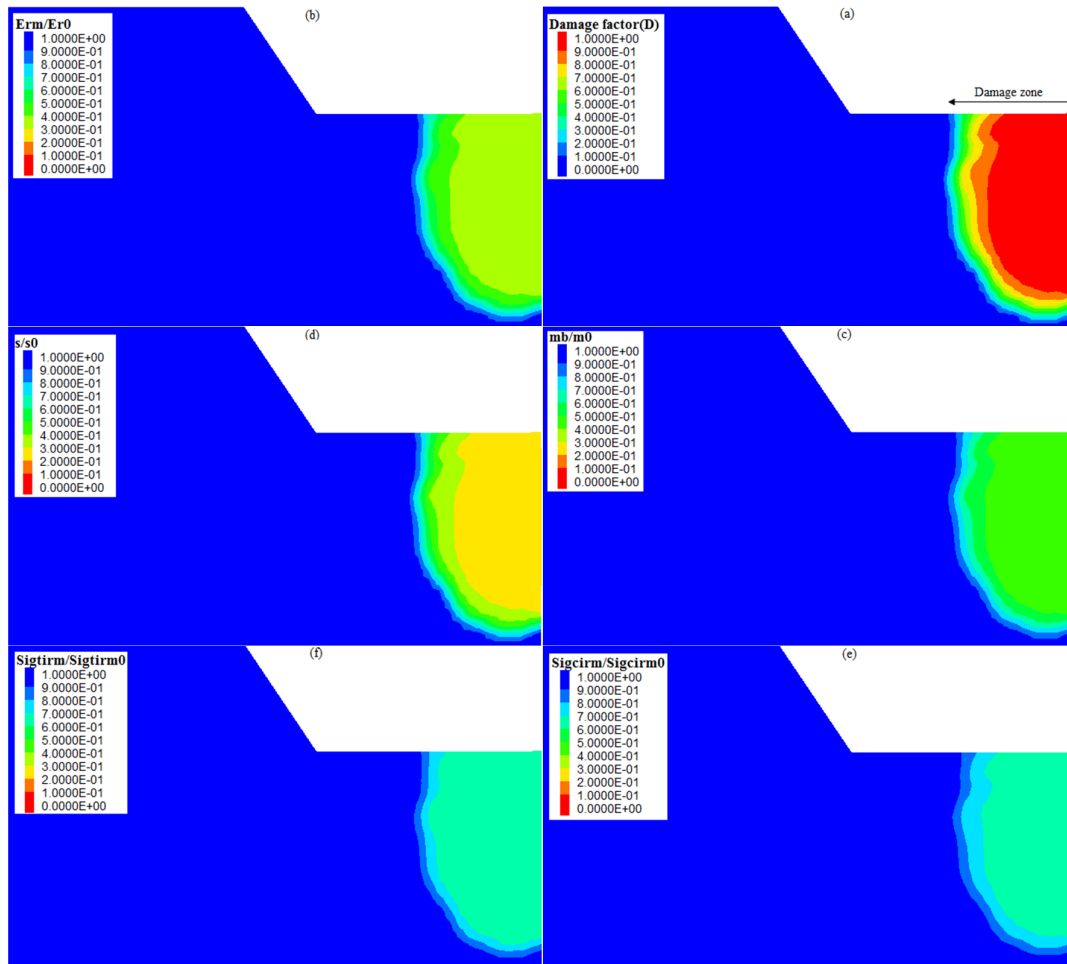


Figure 7. Reduction in rock mass properties in damaged zone (D).

### 4.3. An investigation into plasticity criterion

The plastic zone around the hole can be used as a separate criterion for understanding rock mass fracture behavior due to blast damage and bench health monitoring (BHM). Zones, where stresses satisfy the yield criterion are indicated by the plastic zone around the hole. The plastic yield shows the maximum value of the micro-cracking numerically.

The plastic zone is plotted in Figure 8 and compared with the Hoek-Brown disturbance values as contours. The model was run until the input

wave was totally damped. This was done by recording the history at different points. The plastic zone value was compared with the disturbance zoning of Hoek-Brown at different points until the run was over. The Hoek-Brown damage zoning values approximately equaled the plastic zone. In time  $0.2E-3s$ , when the blasting began, the plastic zone radius equaled  $0.75\text{ m}$ , and the Hoek-Brown damage zoning (D) was  $0.87\text{ m}$ . At the end of the run, the plastic zone radius approximately equaled the Hoek-Brown damage zoning radius around the hole and reached about  $5.5\text{ m}$ , which was around 27 times the model blasting hole radius.



Figure 8. A comparison between plastic zone and D zoning around hole.

### 4.4. An investigation into bench health monitoring (BHM)

The peak particle velocity (PPV), the most common index for judging the value of the rock mass damage, was used for bench health monitoring (BHM) with geometric properties of Figure 5. Figs. 9-11 illustrate the PPV variations in

slope face at three points, i.e. the crest (C), middle (M), and toe (T) of a bench with different heights (H), slopes (a), and widths (distance between the hole and the bench toe, W). Figs. 9-11 demonstrate the short benches ( $H = 5\text{ m}$ ), medium benches ( $H = 10\text{ m}$ ), and high benches ( $H = 15$ ), respectively. Additionally, the history point was considered 1 meter above the bench toe.

It is obvious that the PPV values were reduced with the rise in the hole distance from the slope, i.e. in higher blasting loads (distances closer to the blasting hole), the PPV values increase, and in lower blasting loads (distances far from the blasting hole), the PPV values decline. The PPV value is maximum in the toe and minimum in the crest.

As mentioned in Section 4-2, the damage threshold value of 50 mm/s was selected for calculating safe distances and BHM and drawn as horizontal dashed lines in the figures. As it is visible in Figure 9, in smaller benches where the height is equal to 5 meters, the toe, the middle and the crest of the bench are all within the damage threshold. If the distance between the hole and the

upper bench is about 2 meters, the effect of the vibration and damage will reach the crest of the upper bench. The toe of the upper bench will be damaged if a blast hole is located closer than 6 meters away from it. Therefore, to keep the upper bench safe, either a smaller blast load should be applied or the blast hole should be farther than 6 meters. Also greater vibrations will be recorded, at smoother slopes, i.e. 55 degrees, than at steeper slopes such as 75 degrees. The damage extends to the middle of a medium bench (Figure 10), while it only reaches the toe of a high bench (Figure 11). Furthermore, the PPV values are lower for steeper slopes in constant blasting loads (constant distance between the hole and bench) and are higher for smoother slopes.

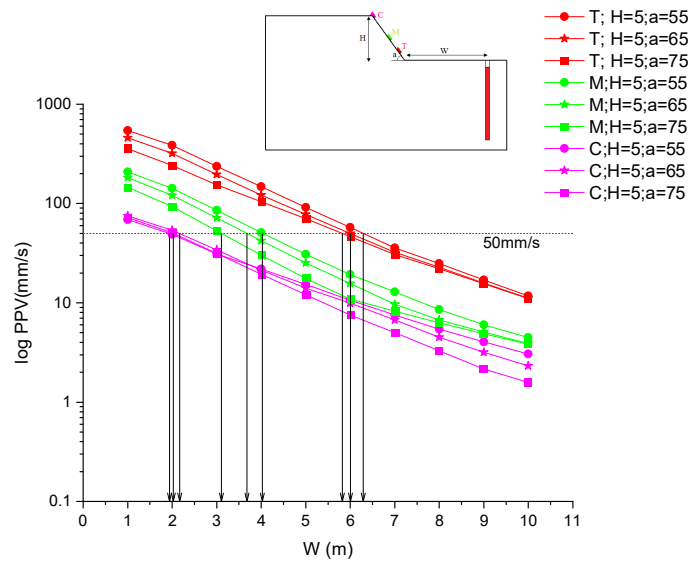


Figure 9. PPV monitoring in toe, middle, and crest of short benches.

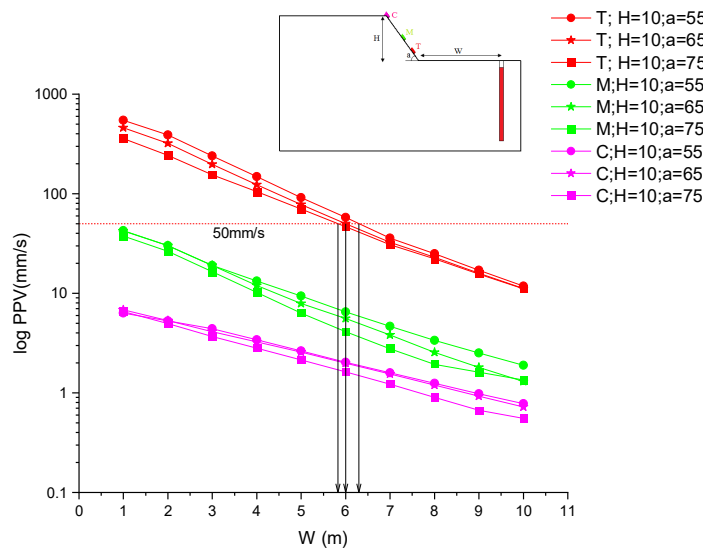


Figure 10. PPV monitoring in toe, middle, and crest of medium benches.

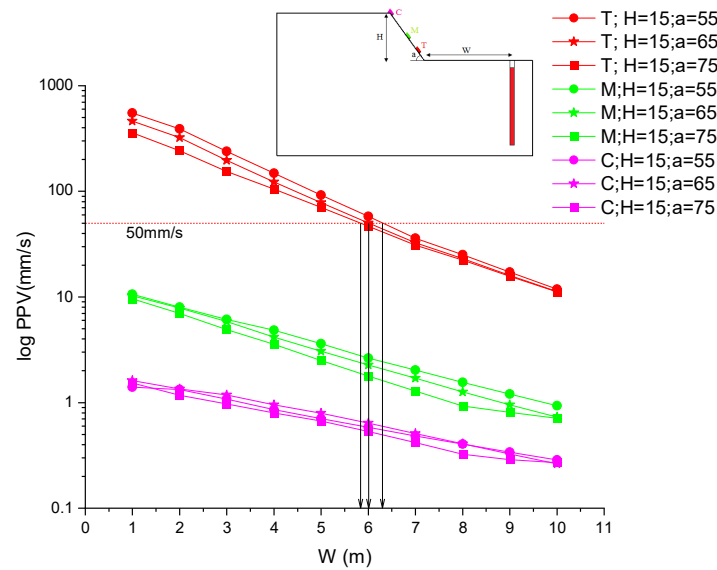


Figure 11. PPV monitoring in toe, middle, and crest of high benches.

## 5. Conclusions

The dynamic capabilities of the finite difference method allow for investigating the mechanism of creation and propagation of waves caused by blasting, expansion of blasting damage zone in the rock mass, and bench health monitoring (BHM). In this work, the blasting process of a granite rock slope was simulated using the Hoek-Brown criterion, and bench health monitoring was evaluated by analyzing the disturbance factor and monitoring the peak particle velocity. The most important results of the work are as follow:

- In the Hoek-Brown failure criterion, the D disturbance factor is estimated based on a descriptive approach, which is complicated. In this work, a quantitative equation was used based on the elastic damage theory. Regarding the numerical simulation results, when the blasting load is applied to the rock mass, the slope damage level increases over time, resulting in accumulative damage. Finally, a broken zone was formed around the blasting hole.
- To some extent, the disturbance factor  $D = 1.0$  remained constant behind the hole. Then it was reduced nonlinearly. The mechanical properties of the Hoek-Brown behavioral model, as well as the rock mass quality, declined due to the nonlinear reduction of D caused by receding from the hole. In the damaged zone, the s parameter of the Hoek-Brown criterion had the maximum affectability from the blasting and was reduced to 0.25 of its primary

value. Meanwhile, the rock's compressive strength had the minimum affectability and was reduced to 0.62 of its primary value.

- According to a rule of thumb, the plastic zone is 15 to 20 times the hole radius. This value was estimated to be 27 times the hole radius using the numerical method, which is close to the above empirical value.
- The affected blasting zone can be obtained, and the bench health monitoring (BHM) can be investigated using the PPV threshold value. Numerical simulation shows that using different rock mass properties in the blasting zone produces different results in the PPV evaluation of the slope compared to using constant parameters. Regarding the PPV analysis, a large blasting load, i.e. a closer hole to the slope face, can cause severe damages to the bench, and the bench will be safer by reducing the blasting load, i.e. increasing the hole's distance from the slope face.
- In smaller benches ( $H = 5$  m) the toe, the middle and the crest of the benches will be in the damage threshold. In medium-sized benches ( $H = 10$  m), the damage will reach near the middle of the bench, and in high benches ( $H = 15$  m), only the toe of the bench will be damaged. Therefore, in order to keep the upper bench safe, either the distance of the hole from the upper step's toe should be increased or the controlled blasting methods should be deployed to

restrain the blast load and vibrations.

- At a constant blast load (constant distance between the hole and bench), the recorded PPV values are lower for steeper slopes, i.e.  $75^\circ$ , and higher for smoother slopes, i.e.  $55^\circ$ . Therefore, smoother slopes are more susceptible to vibration than steeper slopes.

### Conflicts of interest

The authors declare that they have no competing interests.

### Acknowledgment

The authors would like to thank Dr. Mohsen Mohebbi for his constructive and sincere cooperation.

### References

- [1]. Bahadori, M., Bakhshandeh Amnieh, H., and Khajezadeh, A. (2016). A new geometrical-statistical algorithm for predicting two-dimensional distribution of rock fragments caused by blasting. *International Journal of Rock Mechanics and Mining Sciences*. 86: 55-64.
- [2]. Siamaki, A. and Bakhshandeh Amnieh, H. (2016). Numerical analysis of energy transmission through discontinuities and fillings in Kangir Dam. *Journal of Mining and Environment*. 7 (2): 251-259.
- [3]. Jimeno, C.L., Jimeno, E.L., Carcedo, F.J.A., and De Ramiro, Y.V. (1995). *Drilling and blasting of rocks*. CRC Press, London, 408 p.
- [4]. Haghnejad, A., Ahangari, K., Moarefvand, P., and Goshtasbi, K. (2018). Numerical investigation of the impact of geological discontinuities on the propagation of ground vibrations. *Geomech Eng*. 14 (6): 545-552.
- [5]. Kutter, H. and Fairhurst, C. (1971). On the fracture process in blasting, in *International Journal of Rock Mechanics and Mining Sciences and Geomechanics Abstracts*, Elsevier.
- [6]. Lak, M., Fatehi Marji, M., Yarahamdi Bafghi, A., and Abdollahipour, A. (2019). Discrete element modeling of explosion-induced fracture extension in jointed rock masses. *Journal of Mining and Environment*. 10 (1): 125-138.
- [7]. Chamanzad, M.A. and Nikkhah, M. (2020). Sensitivity Analysis of Stress and Cracking in Rock Mass Blasting using Numerical Modelling. *Journal of Mining and Environment*. 11 (4): 1141-1155.
- [8]. Haeri, H., Sarfarazi, V., and Fatehi Marji, M. (2022). Static and Dynamic Response of Rock Engineering Models. *Iranian Journal of Science and Technology, Transactions of Civil Engineering*. 46 (1): 327-341.
- [9]. Sarfarazi, V., Asgari, K., and Abad, M.B. (2021). Interaction between Tunnel and Surface Foundation using PFC2D. *Journal of Mining and Environment*. 12 (3): 785-798.
- [10]. Sarfarazi, V. and Asgari, K. (2022). Influence of Single Tunnel and Twin Tunnel on Collapse Pattern and Maximum Ground Movement. *Journal of Mining and Environment*. 13 (1): 117-128.
- [11]. Saiang, D. (2010). Stability analysis of the blast-induced damage zone by continuum and coupled continuum-discontinuum methods. *Engineering Geology*. 116 (1-2): 1-11.
- [12]. Behera, S. and Dey, K. (2022). A PPV-Based Prediction Model to Construct Damage Envelop for Crater Blasts. *Journal of The Institution of Engineers (India): Series D*. 103 (1): 13-23.
- [13]. Silva, J., Worsey, T., and Lusk, B. (2019). Practical assessment of rock damage due to blasting. *International Journal of Mining Science and Technology*. 29 (3): 379-385.
- [14]. Ataei, M. and Sereshki, F. (2017). Improved prediction of blast-induced vibrations in limestone mines using Genetic Algorithm. *Journal of Mining and Environment*. 8 (2): 291-304.
- [15]. Bakhshandeh Amnieh, H., Mohammadi, A., and Mozdianfard, M. (2013). Predicting peak particle velocity by artificial neural networks and multivariate regression analysis-Sarcheshmeh copper mine, Kerman, Iran. *Journal of Mining and Environment*. 4 (2): 125-132.
- [16]. Pan, Q., Zhang, J., and Zheng, S. (2020). Study on distribution characteristics of damage range along smooth blasting hole based on PPV. *Mathematical Problems in Engineering*.
- [17]. Afrasiabian, B., Ahangari, K., and Noorzad, A. (2020). Study on the effects of blast damage factor and blast design parameters on the ground vibration using 3D discrete element method. *Innovative Infrastructure Solutions*, 5(2), 1-14.
- [18]. Shadabfar, M., Gokdemir, C., Zhou, M., Kordestani, H., and Muho, E.V. (2020). Estimation of damage induced by single-hole rock blasting: A review on analytical, numerical, and experimental solutions. *Energies*. 14 (1): 29.
- [19]. Zheng, H., Li, T., Shen, J., Xu, C., Sun, H., and Lü, Q. (2018). The effects of blast damage zone thickness on rock slope stability. *Engineering Geology*, 246, 19-27.
- [20]. Hoek, E. and Karzulovic, A. (2000). Rock mass properties for surface mines. *Slope Stability in Surface Mining*, WA Hustrulid, MK McCarter and DJA van Zyl, Eds, Society for Mining, Metallurgical and Exploration (SME), Littleton, CO, 59-70.

- [21]. Qian, Z., Li, A.-J., Lyamin, A., and Wang, C. (2017). Parametric studies of disturbed rock slope stability based on finite element limit analysis methods. *Computers and Geotechnics*, 81, 155-166.
- [22]. Sheng, Q., Yue, Z., Lee, C., Tham, L., and Zhou, H. (2002). Estimating the excavation disturbed zone in the permanent shiplock slopes of the Three Gorges Project, China. *International Journal of Rock Mechanics and Mining Sciences*. 39 (2): 165-184.
- [23]. Sanei, M., Faramarzi, L., Fahimifar, A., Goli, S., Mehinrad, A., and Rahmati, A. (2015). Shear strength of discontinuities in sedimentary rock masses based on direct shear tests. *International Journal of Rock Mechanics and Mining Sciences*, 75, 119-131.
- [24]. Hoek, E. and Brown, E.T. (1980). Empirical strength criterion for rock masses. *Journal of the geotechnical engineering division*. 106 (9): 1013-1035.
- [25]. Hoek, E., Carranza-Torres, C., and Corkum, B. (2002). Hoek-Brown failure criterion-2002 edition. *Proceedings of NARMS-Tac*. 1 (1): 267-273.
- [26]. Hoek, E. (2012). Blast damage factor D. Technical note for RocNews, 1-7.
- [27]. Hoek, E. and Brown, E. (2019). The Hoek–Brown failure criterion and GSI–2018 edition. *Journal of Rock Mechanics and Geotechnical Engineering*. 11 (3): 445-463.
- [28]. Li, A., Merifield, R., and Lyamin, A. (2011). Effect of rock mass disturbance on the stability of rock slopes using the Hoek–Brown failure criterion. *Computers and Geotechnics*. 38 (4): 546-558.
- [29]. Yilmaz, M., Ertin, A., Er, S., and Tugrul, A. (2018). Numerical modelling of steep slopes in open rock quarries. *Journal of the Geological Society of India*. 91 (2): 232-238.
- [30]. Lupogo, K., Tuckey, Z., Stead, D., and Elmo, D. (2014). Blast damage in rock slopes: potential applications of discrete fracture network engineering, in *Proceedings of the 1st International Discrete Fracture Network Engineering Conference*, Vancouver, Canada. p.
- [31]. Rose, N., Scholz, M., Burden, J., King, M., Maggs, C., and Havaej, M. (2018). Quantifying transitional rock mass disturbance in open pit slopes related to mining excavation, in *Proceedings of the XIV International Congress on Energy and Mineral Resources*.
- [32]. Lemaitre, J. (2012). *A course on damage mechanics*. Springer Science and Business Media, Berlin, 228 p.
- [33]. Hamdi, E., Romdhane, N.B., and Le Cléac'h, J.-M. (2011). A tensile damage model for rocks: application to blast induced damage assessment. *Computers and Geotechnics*. 38 (2): 133-141.
- [34]. Chen, Y., Xu, J., Huo, X., and Wang, J. (2019). Numerical simulation of dynamic damage and stability of a bedding rock slope under blasting load. *Shock and Vibration*.
- [35]. Wang, Y., Wang, S., Zhao, Y., Guo, P., Liu, Y., and Cao, P. (2018). Blast induced crack propagation and damage accumulation in rock mass containing initial damage. *Shock and Vibration*.
- [36]. Yang, J., Dai, J., Yao, C., Jiang, S., Zhou, C., and Jiang, Q. (2020). Estimation of rock mass properties in excavation damage zones of rock slopes based on the Hoek-Brown criterion and acoustic testing. *International Journal of Rock Mechanics and Mining Sciences*, 126, 104192.
- [37]. Hoek, E. and Brown, E. (1980). *Underground Excavation in Rock: Institute of Mining and Metallurgy*. London, UK.
- [38]. Renani, H.R. and Cai, M. (2021). Forty-Year Review of the Hoek–Brown Failure Criterion for Jointed Rock Masses. *Rock Mechanics and Rock Engineering*, 1-23.
- [39]. Hoek, E. (2007). *Practical rock engineering: RocScience*.
- [40]. Hoek, E. and Diederichs, M.S. (2006). Empirical estimation of rock mass modulus. *International journal of rock mechanics and mining sciences*. 43 (2): 203-215.
- [41]. Zuo, J. and Shen, J. (2020). *The Hoek-Brown Failure Criterion-From Theory to Application*. Springer, Singapore, 225 p.
- [42]. Bhandari, S. (1997). *Engineering rock blasting operations*. Balkema, Rotterdam.
- [43]. Xiao, Y.-X., Feng, X.-T., Hudson, J.A., Chen, B.-R., Feng, G.-L., and Liu, J.-P. (2016). ISRM suggested method for in situ microseismic monitoring of the fracturing process in rock masses. *Rock Mechanics and Rock Engineering*. 49 (1): 343-369.
- [44]. Hoek, E. and Brown, E.T. (1997). Practical estimates of rock mass strength. *International journal of rock mechanics and mining sciences*. 34 (8): 1165-1186.
- [45]. Kuhlemeyer, R.L. and Lysmer, J. (1973). Finite element method accuracy for wave propagation problems. *Journal of the Soil Mechanics and Foundations Division*. 99 (5): 421-427.
- [46]. Itasca, F. (2012). *Fast Lagrangian Analysis of Continua in 3-Dimension (FLAC3D V 5.01)*. Itasca Consulting Group: Minneapolis, MN, USA.
- [47]. Grisaro, H.Y. and Edri, I.E. (2017). Numerical investigation of explosive bare charge equivalent weight. *International Journal of Protective Structures*. 8 (2): 199-220.

## بررسی پایش سلامت پله معدن تحت بارگذاری انفجار در معیار شکست هوک-براون به روش تفاضل محدود

سیداحمد موسوی<sup>۱</sup>، کاوه آهنگری<sup>۱\*</sup> و کامران گشتاسبی<sup>۲</sup>

۱- بخش مهندسی معدن، دانشگاه آزاد اسلامی واحد علوم و تحقیقات، تهران، ایران

۲- بخش مهندسی معدن، دانشکده فنی و مهندسی، دانشگاه تربیت مدرس، تهران، ایران

ارسال ۲۰۲۲/۰۷/۱۰، پذیرش ۲۰۲۲/۰۹/۰۷

\* نویسنده مسئول مکاتبات: ahangari@srbiau.ac.ir

### چکیده:

انفجار و رهاسازی تنش باعث ایجاد ترک، شکستگی و ایجاد ناحیه آسیب حفاری در توده‌سنگ باقی‌مانده می‌شود. پایش سلامت پله معدن (BHM) از نظر ایمنی و سلامت پله در بارگذاری دینامیکی انفجار بسیار حائز اهمیت است. به‌منظور برآورد سریع مشخصات مختلف توده‌سنگ در ناحیه آسیب ناشی از انفجار، برخی از معیارهای تجربی پیشنهاد شده است. این مطالعه خواص توده‌سنگ پشت چال انفجاری را بر اساس معیار شکست هوک-براون تعمیم یافته و ضریب آسیب کمی (D) تخمین می‌زند. در نظر گرفتن مقدار D به صورت یک عدد ثابت برابر صفر و یا یک، برای کل توده‌سنگ، مقاومت و پایداری توده‌سنگ را تا حد زیادی دستخوش تغییر قرار می‌دهد و تحلیل‌ها یا می‌توانند خیلی خوشبینانه باشد و یا خیلی محافظه کارانه. بنابراین با در نظر گرفتن مقدار کمی D بر اساس تئوری آسیب الاستیک، به‌جای یک مقدار ثابت در ناحیه آسیب دیده، شبیه سازی عددی بر اساس برنامه تفاضل محدود FLAC برای ارزیابی میزان لرزش و آستانه آسیب با رصد کردن بیشینه سرعت ذره‌ای (PPV) در دامنه پله با ژئومتری‌های مختلف انجام گرفت. شبیه‌سازی عددی نشان می‌دهد که با افزایش عمق در پشت چال انفجاری، مقدار D از ۱ به ۰ تقریباً به صورت غیر خطی کاهش می‌یابد و متعاقباً خصوصیات توده‌سنگ مربوط به مدل رفتاری هوک-براون به صورت غیر خطی کاهش می‌یابد. مشخص شده است که با استفاده از پارامترهای مختلف توده‌سنگ در ناحیه آسیب ناشی از انفجار در پشت چال، مقدار PPV کاملاً متفاوت از پارامترهای ثابت به‌دست می‌آید. بنابراین، رویکرد استفاده از مقدار کمی ضریب D، برای تخمین سریع ویژگی‌های مختلف توده‌سنگ در ناحیه آسیب انفجار و همچنین محاسبه میزان لرزش، بسیار حائز اهمیت است.

**کلمات کلیدی:** ضریب آسیب (D)، پایش سلامت پله (BHM)، معیار شکست هوک-براون، بیشینه سرعت ذره‌ای (PPV)، ناحیه پلاستیک، ژئومتری شیب.